ELASTIC PLASTIC CRACK ANALYSIS BY FINITE ELEMENT METHOD UNDER MIXED MODE LOADING CONDITIONS

Aidy Ali[1], Ahmed Kamal Ariffin[2], Muhammad Rawi Mohamed Zin[2], Mohd Sapuan Salit[1*], Mhd Yunin Hassan[1] and Mohd Rasid Osman[1]

Received: Jun 5, 2003; Revised: Mar 9, 2004; Accepted: Mar 18, 2004

Abstract

The modeling of crack growth in ductile material is presented in this paper. The direction of the crack is assumed to follow the maximum principle normal stress. The material is modeled to be of elastic-plastic behavior and the fracture criterion used is Rice's *J*-Integral. The crack is modeled to start from a rectangular notch and propagation of the crack tip is represented by the deleted element mechanism. The crack growth direction was validated by experiments and good agreement with the simulation is observed.

Keywords: Crack growth, *J*-integral, deleted element, simulation

Introduction

There has been much interest in the analysis of mixed-mode fracture over many years. Direction of mixed mode crack propagation model has been characterized by many direction criteria such as maximum tensile stress (Erdogan and Shih, 1993), minimum strain energy density (Shih, 1974), maximum tangent stress and maximum shear stress (Dsekmann *et al.,* 1992) and maximum principle stress (Smith, 1987). These criteria were combined with fracture criteria such as a stress intensity factor, crack tip opening displacement (CTOD) or crack tip opening angle (CTOA) and *J*-Integral. However, Waryznek (1991) mentioned that none of these fracture criteria and direction criteria could represent the crack propagation behaviors.

The combination of fracture criteria with the appropriate direction criteria is still under investigation. James (1998) has combined CTOD with maximum tensile stress to model the crack growth in elastic-plastic material behavior. The crack growth mechanism used was the nodal release and remeshing technique. Similar work has been carried out by Waryznek (1991). Hoff *et al*. (1986) discussed in detail the most popular crack growth mechanism in finite element methods. Besides the released node and remeshing techniques, Liu (1998) implemented zero stiffness at elements, which was involved in the crack path. Nasir (1988) used a different crack propagation mechanism where the crack tip is located at patch elements, which were pasted

[1*] *Department of Mechanical and Manufacturing Engineering, Universiti Putra Malaysia, 43400 Serdang, Selangor, Malaysia. E-mail:sapuan@eng.upm.edu.my*

[2] *Department of Mechanical and Materials EngineeringUniversiti Kebangsaan Malaysia, 43400, Bangi, Selangor, Malaysia*

[*] *corresponding author*

Suranaree J. Sci. Technol. 11:91-96

to the background elements. The patch elements are moved when the crack tip changed its location.

In this paper the deleted element mechanism to simulate the crack propagation and coupling it with *J*-Integral (Rice and Rosengren, 1968) is proposed as the fracture criterion and the maximum principle stress criterion as the direction criterion.

Materials and Methods

The material is assumed to be ductile and it has been modeled to be of elastic-plastic behavior. Yield stress is characterized by the von Mises yield criterion as shown in equation (1) below and it follows the J_2 incremental plasticity theory and is in accordance with the associated flow rule.

$$\sigma_{vm}^2 = 3\left[\frac{1}{2}\left(\sigma_x^2 + \sigma_y^2\right) + \tau_{xy}^2\right] \quad (1)$$

where σ_x, σ_y and τ_{xy} are normal in the x direction, normal stress in the y direction and shear stress respectively.

The elastic-plastic hardening characteristics were modeled by piecewise linear function of the form $\bar{\sigma} = \sigma_y + H\left(\bar{\varepsilon}_p\right)$, where, $\bar{\sigma}$ and $\bar{\varepsilon}_p$ are effective stress and effective plastic strain respectively. H is a hardening parameter.

In the incremental plasticity theory, stress-strain relation of the material is given by $d\sigma = D_{ep}\, d\varepsilon$, where D_{ep} is the tangent modulus given in equation (2) and D_e is the elastic modulus.

$$D_{ep} = \left[D_e - \frac{\left\{\frac{\partial f}{\partial \sigma}\right\}\left\{\frac{\partial f}{\partial \sigma}\right\}^T}{\frac{1}{d\lambda}\frac{\partial Y}{\partial_K} d_K + D_e\left\{\frac{\partial f}{\partial \sigma}\right\}\left\{\frac{\partial f}{\partial \sigma}\right\}^T} \right] \quad (2)$$

The specimen containing a rectangular notch is modeled as shown in Figure 1. Load is applied to the upper side nodes. The loading angle is calculated by equation (3).

$$\beta = \tan^{-1}\left(\frac{F_x}{F_y}\right) \quad (3)$$

where, F_x, F_y and F (Figure 1) are forces in the x direction, y direction and resultant force respectively. The bottom side is fixed where the displacement U is equal to zero. The material properties of modeling is summarized in Table 1, where the Young's modulus E is 71,700 MPa, Poisson's ratio is 0.33, strain hardening parameter is 996.63 MPa, critical fracture toughness is 400 N/mm, and yield stress is 179.27 MPa.

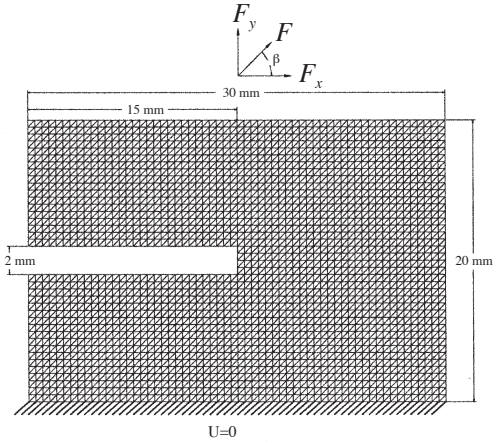

Figure 1. Finite element model.

Table 1. Material properties of specimen.

Young's modulus, E (MPa)	71,700
Poisson's ratio, v	0.33
Strain hardening parameter, H (MPa)	996.63
Critical fracture toughness, J_c (N/mm)	400
Yield stress, σ_y (MPa)	179.27

Fracture Toughness, J_c is assumed to be a universal variable which can be used to characterize the fracture behavior in the mixed mode (mode *I* and mode *II*) loading. The finite element model is loaded in incremental. The *J*-integral is calculated along the integration path for each load increment and is compared with J_c. The crack starts when the calculated *J*-integral has reached or is larger than J_c. *J*-integral is calculated using equation (4) and equation (5), where these particular equations represent the plastic *J* component and the elastic *J* component respectively.

$$J_e = \left[\left(\frac{1}{2E}\left(\sigma_x + \sigma_y\right)^2\right) + \left(\frac{1+\upsilon}{E}\right)\left(\tau_{xy} - \sigma_x\sigma_y\right)\right]\int_\Gamma dy \quad (4)$$

$$J_p = \left[\left(\sigma_x + \tau_{xy}\right)\left(\tau_{xy} + \sigma_y\right) + \begin{Bmatrix}\left(\frac{1}{\det J}\right)^2\left(y_{23}\left(q_1 - q_5\right) - y_{13}\left(q_3 - q_5\right)\right)\\ \left(y_{23}\left(q_1 - q_6\right) - \left(y_{13}\left(q_4 - q_6\right)\right)\right)\end{Bmatrix}\right]\int_\Gamma ds \quad (5)$$

Integration path, Γ is allowed to follow the one-element length around the crack tip node. The node labelled with "G" represents the initial notch tip (Figure 2 (A)) and the first crack tip (Figure 2 (B)) as shown in Figure 2. The crack tip is assumed to be the node where a maximum value of principle stress is compared to the other nodes. The integration path is searched automatically during the growth of the crack tip. This can be illustrated in Figure 2 where the integration path for the initial notch is $A \rightarrow B \rightarrow C \rightarrow D \rightarrow E \rightarrow F$ in Figure 2 (A) and the one for the first crack is $A \rightarrow B \rightarrow C \rightarrow D \rightarrow E \rightarrow F$ in Figure 2 (B).

The load increases until the crack starts. Then, the crack growth is modeled by the deleted element mechanism. In this mechanism, the element with the maximum principle stress is deleted. A new crack tip node is defined when the crack element is deleted from the mesh data. The crack is propagated for every new crack tip created.

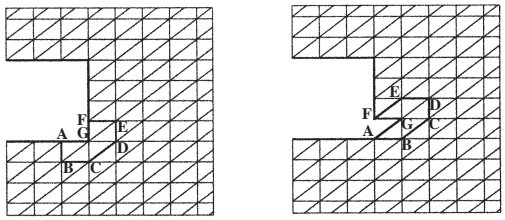

(A) (B)

Figure 2. Integration path for initial notch and first crack.

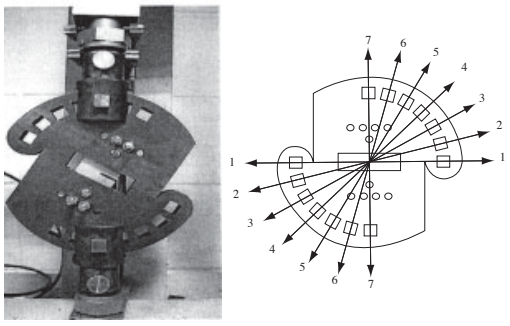

(A) (B)

Figure 3. Test rig for mixed mode.

Besides the simulation, the mixed mode experiments were conducted to validate the crack growth direction model. The specimen shown in Figure 1 was clamped to the mixed mode fixture as shown is Figure 3 (A). The specimen was loaded at mode *I* if the tensile load applied is parallel to hole #7, and mode *II* if it is parallel to hole #1. Furthermore, the specimen was loaded in mixed mode condition when it was pulled from hole #2 to hole #6, where, the angle between the holes is 15 degree. These are shown in Figure 3 (B).

Results and Discussion

The dimension of the modeled plate portion is 20 mm in height, 30 mm in width and 2 mm in thickness. However, the actual dimension of the specimen is 80 mm in height, 30 mm in width and 2 mm in thickness. The size of the initial notch is 2 mm in height and 15 mm in width as shown in Figure 1 for the finite element model. The specimen was loaded at 15^{o}, 30^{o} angles respectively. The results from the experiment are shown in Figure 4 and those from the simulation are shown in Figure 5.

It can be seen that, the crack started at the lower sharp corner of the rectangular notch as shown in Figures 4 and 5. The results from the experiments show the crack propagated at about a 45^{o} angle down from the notch and it changed the direction to almost a flat path until the total fracture. However, the simulation does not show the fracture. Before changing the direction to a flat path, the crack is influenced by the mixed mode condition. On the other hand, when it has propagated to a flat direction, it is influenced by mode *I*. This shows that the cracks tend to change from the mixed mode *I* and *II* condition to the mode *I* propagation as illustrated in Figures 4 and 5.

Figure 6 shows the comparison of the crack path for loading at 15^{o}, 30^{o} and 60^{o} angles. Before the crack growth direction changes at 30^{o} and 60^{o} angles, the crack path is almost the same. However, the crack caused by the loading at the 30^{o} angle can be compared to the growth direction at the 60^{o} angle. James (1998) also observed this similar behavior in his analysis

from a pre-cracked specimen model.

The behavior of crack length with load is shown in Figure 7. At the initial stage, up to a crack length of about 3 mm, the crack was propagated by increasing loads. However, when the crack length is larger than 3 mm, the crack occurs at decreasing loads. If the crack length is larger than 10 mm, load causing crack is smaller for the 30° and 60° loading angles compared to the 15° loading angle. This behavior is in accordance with the work carried out by James (1998) and Waryznek (1991).

Figure 8 shows the *J*-integral versus load for 15°, 30° and 60° loading angles from the initial crack. J_c from Table 1 is 400 N/mm. Crack is initiated when the calculated *J* is larger than J_c as shown in Figure 7. The maximum load is about 800 N for 15°, 1,000 N for 30°and 1,100 N for 60° loading angles. The loads mentioned above are the resultant value of horizontal and vertical forces. Increasing F_y means increasing the mode *II* loading. It could be concluded that, mode *II* dominated crack requires lower load compared to mode *I* dominated crack.

The stress-strain curve before crack for elements close to the rectangle notch is shown in Figure 9. The gradients of the curve for 15, 30 and 60° angles are similar due to the same value of Young's modulus used in the elastic-plastic behavior of the ductile material. The fracture started at different stresses for each loading angle, where a larger loading angle requires bigger stress to fracture. The results of stress-strain at fracture are tabulated in Table 2.

Conclusions

The important conclusions of this work are summarized below.

1. The deformed surface of a notch in a ductile material subjected to mixed-mode (combination of modes *I* and *II*) loading shows blunting along a certain portion and sharpening of the notch becomes very acute.
2. For β in the range from 0° to 15°, failure of the ligaments occurs by propagation of a shear crack. This is caused by an accumulation of intense shear deformation

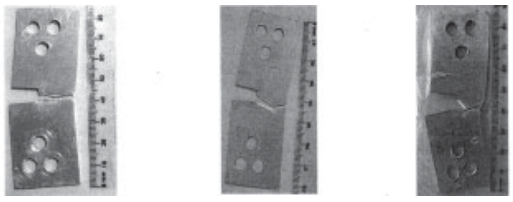

15° 30° 60°

Figure 4. Result for loading at 15°, 30° and 60° angles from the experiment.

Table 2. Stress-strain at fractured.

Loading angle (degree)	Stress (MPa)	Strain
15	1,060	0.84
30	1,475	1.24
60	1,892	1.64

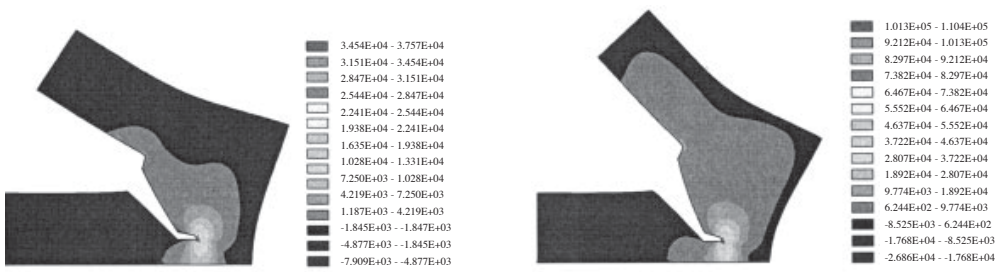

30° 60°

Figure 5. Result from simulation for loading at 30° and 60° angles.

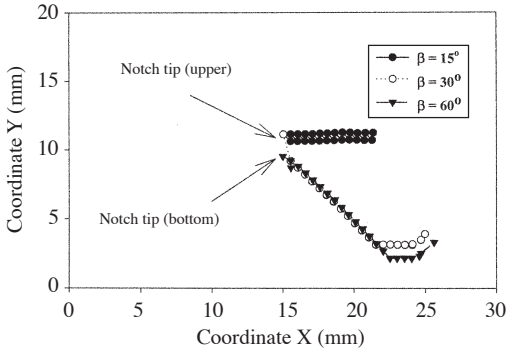

Figure 6. Crack path for 15°, 30° and 60°.

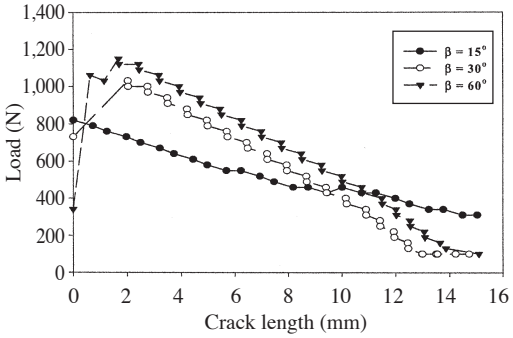

Figure 7. Load versus crack length.

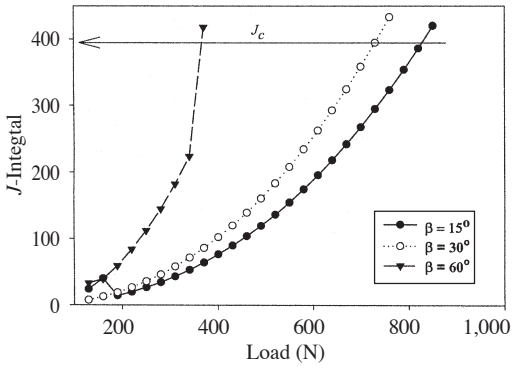

Figure 8. *J*-intergral versus load.

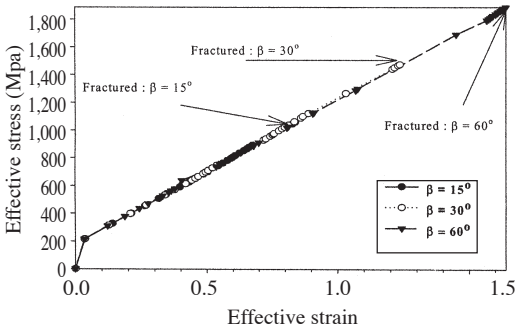

Figure 9. Stress-strain curve.

within a narrow band which emanates from the sharpened part of the notch.

3. For β in the range from 30° to 60°, failure of the ligament connecting the deformed notch tip with the hole occurs by the classic void sheet mechanism.
4. The critical value of J at ductile fracture initiation decreases as β is reduced from 90°, reaches a minimum at around β = 30° and thereafter increases sharply for further reduction in β. This trend has been rationalized by Ghosal and Narasimban (1996) after they carefully examined the plastic strain accumulation and the magnitude of hydrostatic stress in the ligament.

This research has successfully modeled the crack growth behavior from a rectangular notch of ductile material where it is assumed to exhibit elastic-plastic behavior. The *J*-integral is successfully used for mixed mode fracture and maximum principle stress is a good crack propagation direction criterion.

References

Dsekmann, P., Pawliska, P., and Richard, H.A. (1992). Elastic plastic crack analysis under mixed mode loading conditions. International Journal of Fracture, 57:249-252.

Erdogon, F., and Shih, G.C. (1993). Maximum tensile stress criterion. Journal of Basic Engineering, 85:519-527.

Ghosal, A.K., and Narasimhan, R. (1996). Numerical simulation of hole growth and ductile fracture initiation under mixed-mode loading. International Journal of Fracture, 77:281-304.

Hoff, R., Rubin, C.A., and Hahn, G.T. (1986). A new finite element technique for modeling stable crack growth. Engineering Fracture Mechanics, 23:105-118.

James, M. (1998). A plane stress finite element model for elastic-plastic mode I/II crack growth, [Ph.D. Thesis]. University of Kansas State, USA.

Liu, A.F. (1998). Structural life assessment method. ASM International.

Nasir, T. (1988). Elasto-plastic finite element

formulation and numerical study of a compact tension (CT) fracture specimen. Buletin Jentera, 7:53-67.

Rice, J.R., and Rosengren, G.F. (1968). Plane strain deformation near a crack tip in a power-law hardening material. Journal of Mechanical, Physic and Solid, 16(1): 1-12.

Shih, G.C. (1974). Minimum strain energy density. International Journal of Fracture, 10:305-321.

Smith, R.N.L. (1987). Maximum principle stress. Engineering Fracture Mechanics, 26:463-469.

Waryznek, P. (1991). A two-dimensional crack propagation simulator. International Journal of Fracture, 6:281-304.